



Ministry of Science, Research & Technology  
Iranian Research Organization  
for Science and Technology

## The effect of initiator and weight ratio on dynamic-mechanical properties of multilayer latex IPN with core/shell morphology

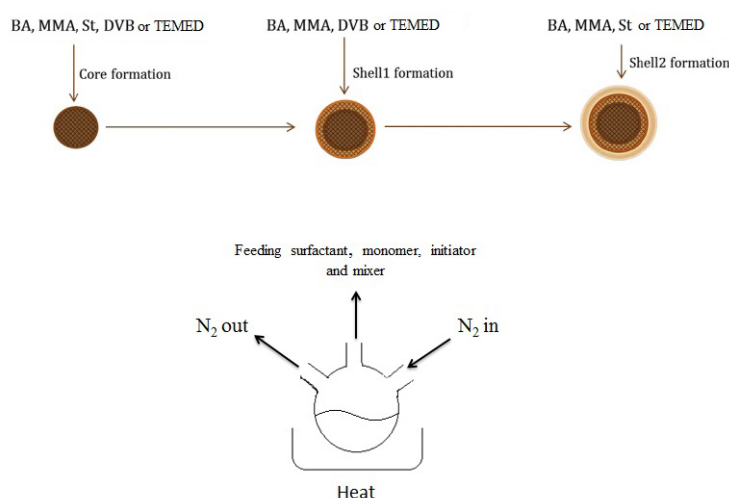
Seyedeh Maedeh Azadeh Ghahfarokhi\*, Iraj Amiri Amraei

Composite Research Center, Malek Ashtar University of Technology, Tehran, Iran

### HIGHLIGHTS

- Interpenetrating polymer networks with core/shell morphology confirm their high damping capacity ( $\tan\delta > 0.3$  and damping temperature range  $> 100^\circ\text{C}$ ).
- The IPN core/shell latex particles with a thermal initiator exhibited the best damping properties.
- By changing the weight ratio of the layers and the amount of PBA in the last layer, the effective damping range increases.

### GRAPHICAL ABSTRACT



### ARTICLE INFO

#### Article history:

Received 15 December 2020

Revised 22 February 2022

Accepted 10 March 2022

#### Keywords:

Damping  
Dynamic-mechanical analysis  
Multilayer core/shell  
Redox  
Thermal

### ABSTRACT

Polymers have good dynamic mechanical properties and high damping capacity due to their viscoelastic nature, especially in the glass transition range, and are considered a good damper with a loss factor greater than 0.3 and a peak temperature range of at least 60-80°C. Two of the best ways to expand the damping range are fabricating the core/shell latex particles with a specific morphology and using interpenetrating polymer networks in the core and shell sections. The aim of this study is to synthesize and investigate the dynamic-mechanical properties of interpenetrating polymer networks with core/shell morphology. A set of multilayer core/shell/shell latex particles with styrene-acrylic monomers were synthesized by varying the initiator (thermal initiator and redox initiator) via semi-continuous emulsion polymerization. In this study, synthesized particles were characterized with fourier transform infrared (FT-IR) spectroscopy, the morphology was determined by transfer electron microscopy (TEM), and the size and size distribution were investigated via dynamic laser scattering (DLS), which represent nano-scale particles with narrow distribution. The damping properties of the formed films were studied by dynamic mechanical analysis (DMA). The factors affecting the formation of poly(styrene/methyl methacrylate/butyl acrylate)-based core/shell particles, including the type of initiator and layer mass ratio, were discussed. The results showed that the IPN core/shell latex particles with a thermal initiator exhibited the best damping properties, with a broad effective damping range ( $\tan\delta > 0.3$ ). The influence of the layer mass ratio on damping was also explored in this work.

\* Corresponding author: Tel.: +9821-22970173 ; Fax: +9821-22935341 ; E-mail address: [smd.azadeh@gmail.com](mailto:smd.azadeh@gmail.com)

## 1. Introduction

Core/shell latex particles have gained considerable scientific attention to their physicochemical characteristics. They can be used to achieve materials with better properties than their basic homopolymers. Core-shell polymers are employed in numerous applications, including impact toughening [1-3], modifiers [4,5], adhesives [6], damping [7] and in high-technology areas like chemical sensing, biosensors, 3D optical data storage, and security of data encryption [8-10]. A common method for synthesizing core/shell particles is semi-continuous emulsion polymerization. It is also effective to prepare a multilayer polymer latex in which each layer is synthesized in a stepwise manner. A variety of polymers with different morphologies and features can be prepared by controlling the thickness and number of layers, weight ratio of layers, as well as the approach of feeding and swelling level of the layers together.

Polymers exhibit time and temperature-dependent behaviors owing to their viscoelastic properties. Knowledge of the dynamic-mechanical characteristics of a polymer is necessary to choose the appropriate polymer for a particular application. Materials with good damping show a high loss factor ( $\tan \delta > 0.3$ ) over a temperature range of at least 60-80°C [11]. The damping features of a polymer are influenced by its glass transition temperature. Damping can be demonstrated using the dissipated energy as heat during relatively slow deformation of the materials, i.e., fatigue experiments. Damping also provides another mechanism of energy adsorbing, unlike impact resistance. Generally, homopolymers show effective damping properties in a narrow temperature range of 20-30°C around their  $T_g$ . The glass transition can be extended or shifted using grafting, mixing, copolymerization, or the development of inter-penetrating networks (IPNs) [12]. IPNs are made up of a combination of two or more cross-linked polymers whose networks are organized in the presence of the other [13]. The addition of a crosslinking agent in full IPNs (both polymers) or semi-IPNs (one phase) limits the size to a very small domain and increases the formation degree of the microheterogeneous structure, which leads to wide glass transition, making them very effective as damping materials [14-16]. Latex IPNs made by focusing on pure IPN particles (with full or semi IPNs) are currently used in a wide range of

temperature damping materials [17,18].

Until now, only a few studies have been carried out to investigate the dynamic-mechanical and damping characteristics of multilayer core/shell latex particles, especially those with IPN as a core. Zahedi *et al.* synthesized a series of multilayer latex IPNs with styrene-acrylic monomers. They stated that the dynamic-mechanical features of the prepared particles depended on the final layer mass ratio, the amount of cross linker, the monomer feeding method, and the difference between adjacent layers  $T_g$  [19]. Wang and coworkers [15] investigated the damping property of a polystyrene/polyacrylic latex IPN. Their results show that the manner of phase separation and damping properties were affected by an increase in the hydrophobic polymer in the shell and a decrease in the hydrophobic polymer in the core, and vice versa. In another study, Silverstein *et al.* [20] reported on IPN core/shell particles synthesized by styrene and acrylic monomers and investigated their morphology. The relationship between the dynamic-mechanical response and the morphology of particles has been studied.

In this work, latex particles consisting of three layers accompanied with a controlled structure were designed to investigate the damping properties of multilayer core-shell particles. The emulsion polymerization used to synthesize the latex particles was developed in a previous study [19]. The main goal of this study was to synthesize and characterize core/shell latex polymers for toughening thermoplastics and to produce better properties of damping by changing the type of initiator. Dynamicmechanical analysis (DMA) showed a higher peak for the redox initiator in the core/shell/shell particles in comparison to the samples synthesized with a thermal initiator. However, the thermal initiator method provided the widest effective range of damping (temperature range with  $\tan \delta > 0.3$ ). Also, the effective temperature range was improved by enhancing the weight ratio of the layers.

## 2. Experimental

### 2.1. Materials

Butyl acrylate (BA), methyl methacrylate (MMA), and styrene (St) monomers were purchased from Merck Co. and purified with a 10 wt% solution of NaOH. Divinylbenzene (DVB) as crosslinking agent was

purchased from Merck Co. Sodium dodecyl sulfate (SDS) as an anionic surfactant and Sorbitan Oleate (Span80) as a nonionic surfactant were purchased from Merck Co. and Aldrich Co., respectively. Ammonium persulfate (APS), sodium bisulfate (SBS), and Tetramethylethylenediamine (TMEDA) as initiators were purchased from Merck Co. Sodium Bicarbonate as a buffer agent and Hexadecane was purchased from Merck Co. All solutions were prepared with deionized water.

## 2.2. Synthesis of core/shell/shell particles

As listed in Table 1, four samples were synthesized in a process similar to Ref. [16] where particles were prepared layer-by-layer. In this work, the Flory-Fox equation was applied to formulate the monomer's composition of the layers. It is a popular experimental formula where molecular weight is related to the glass transition temperature ( $T_g$ ) in the polymer system according to Eq. (1) [21].

$$(1/T_g) = (W_1/T_{g1}) + (W_2/T_{g2}) \quad (1)$$

where  $W_1$  and  $W_2$  represent weight fractions of components 1 and 2, respectively.

Fig. 1 represents a schematic illustration of the preparation of IPN core/shell particles. In the first stage of polymerization, a 500 ml four-neck glass reactor (round-bottom flask) equipped with a thermocouple, a stirrer, a port for purging  $N_2$ , and an inlet of dropping ingredients was used to carry out polymerizations. First, 100 ml of deionized water, buffer agent, and the calculated amount of surfactants (as in Table 2) were added to the reactor. The reactor content was heated to  $50 \pm 5^\circ\text{C}$  and stirred at 300 rpm under a nitrogen atmosphere for 15 min. Then, the BA, MMA, St monomers, and DVB were introduced to the reactor dropwise at a  $1 \text{ g}\cdot\text{min}^{-1}$  speed. The reactor temperature

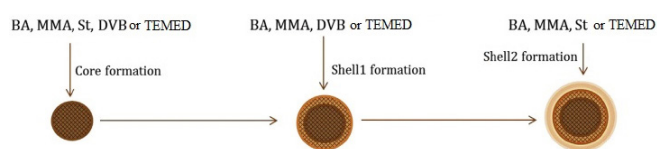


**Fig. 1.** Schematic illustration of the preparation of IPN core/shell particles..

was increased to  $75 \pm 5^\circ\text{C}$ . Next, an aqueous solution of the initiator purified by  $N_2$  atmosphere was added to the system to eliminate the dissolved oxygen, and the speed was increased to 350 rpm. To assure the removal of air, the system was kept under a nitrogen atmosphere for 30 min. Finally, to synthesize the cores, the reactor content was polymerized for 90 min at a temperature of  $75 \pm 5^\circ\text{C}$  with a 350 rpm stirring speed.

In the second stage of polymerization, the second layer of a core/shell structure was made as the shell. In this step, a mixture of the surfactant, the monomers, DVB, and an oxygen-free aqueous solution of initiators was slowly added to the reactor and purified by nitrogen. Then, the mixing speed was raised to 400 rpm, and polymerization was performed for 120 min at  $75 \pm 5^\circ\text{C}$ . All the above stages were accomplished in the final step of the formation of core/shell/shell particles (the second layer of the shell). The stirring rate and temperature were adjusted to 450 rpm and  $75 \pm 5^\circ\text{C}$ , respectively, and polymerization was continued for 8 h. All the above steps were performed to synthesize core/shell/shell particles with a redox initiator at  $40^\circ\text{C}$ , according to Table 3.

In order to prepare a latex film, samples of latex were cast on glass jars (with a 4 mm thickness). At first, samples were dried at room temperature for 48 h and then at  $55^\circ\text{C}$  in the oven for 24 h. In this way, the particles distribution of latex is transformed from diluted to concentrated, then to a packed array, and finally transformed to a continuous polymer film.

**Table 1.** Code and characteristics of synthesized particles.

Sample no.	Temperature ( $^\circ\text{C}$ )	Sample code	Mass ratio (g) Core : shell1 : shell2	Maximum loss factor [ $\tan\delta(\text{max})$ ]	Effective temperature region ( $^\circ\text{C}$ )
1	75	C/S/S-1	1:2:3	0.59, 0.19	174
2	75	C/S/S-2	1:2:2	0.64, 0.21	62
3	75	C/S/S-3	1:3:3	0.58, 0.39	115
4	40	C/S/S-4	1:2:3	0.9, 0.19	86

**Table 2.** The ingredients used for the synthesis of C/S/S-1 sample multilayer core/shell latex particles at 75°C.

Layer	H <sub>2</sub> O (g)	SDS (g)	Span80 (g)	Buffer (g)	HD (g)	BA (g)	MMA (g)	St (g)	DVB (g)	APS (g)	SBS (g)	H <sub>2</sub> O (g)
Core	100	0.37	0.37	0.2	0.9	1	1	13	2.1	0.0512	0.0238	25
Shell 1	9.5	0.6	0.6	0	0.6	13	17	0	4.2	0.0832	0.04	23
Shell 2	7.5	0.145	0.145	0	0.145	28	1	1	0	0.0832	0.04	23

**Table 3.** The ingredients used for the synthesis of C/S/S-4 sample multilayer core/shell latex particles at 40°C.

Layer	H <sub>2</sub> O (g)	SDS (g)	Span80 (g)	Buffer (g)	HD (g)	BA (g)	MMA (g)	St (g)	DVB (g)	TEMED (g)	APS (g)	H <sub>2</sub> O (g)
Core	100	0.48	0.48	0.25	1.125	1	1	13	2.1	0.064	0.064	25
Shell 1	9.5	0.75	0.75	0	0.75	13	17	0	4.2	0.249	0.249	23
Shell 2	10	0.4	0.4	0	0.4	28	1	1	0	0.416	0.416	23

### 2.3. Characterization techniques

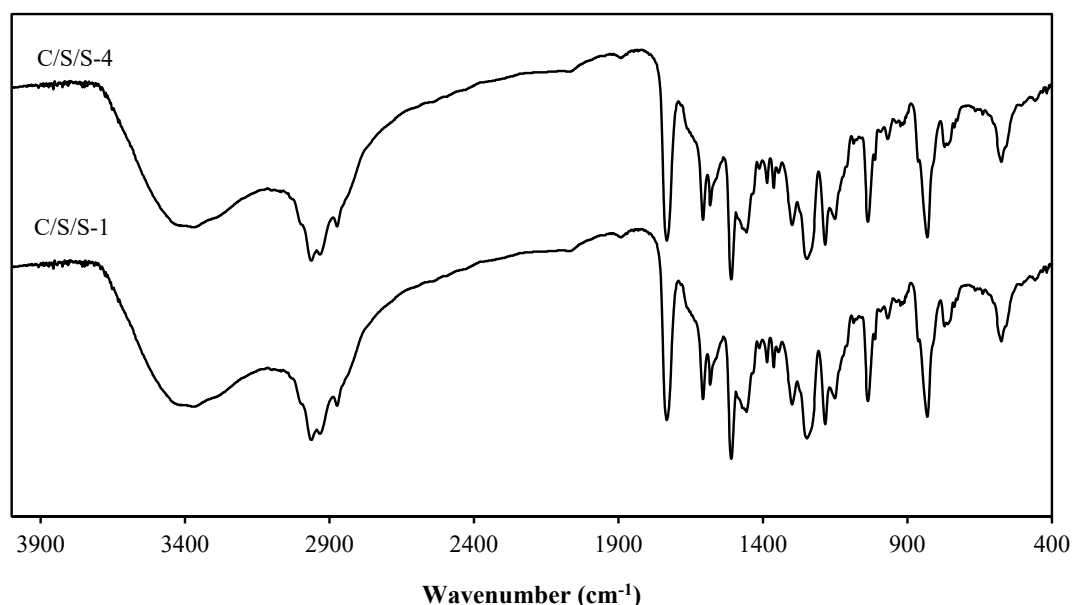
The size distribution of the prepared particles was found by dynamic light scattering (DLS) analysis using a Nano Brook 90Plus Particle Size Analyzer. Fourier transform infrared (FT-IR) spectroscopy was used to investigate the functional groups of the particles. FT-IR spectra were recorded with a Nicolet 800 Fourier transform infrared spectrometer (Thermo Electron Corporation, USA) on a KBr plate (at 4000-400 cm<sup>-1</sup>). The IPN core/shell latex particles were diluted, dispersed, poured on the surface of copper mesh, and then dried at room temperature. Transfer electron microscopy (TEM) was carried out with a Zeiss-EM10C-80 kV (Germany) transmission electron microscope.

DMA (PerkinElmer DMA 8000) was applied to measure the dynamic-mechanical behavior of the films. Parameters including the storage modulus ( $G'$ ), loss modulus ( $G''$ ), and loss factor ( $\tan \delta$ ) were obtained. The curve of the loss factor temperature was recorded at a frequency of 1 Hz and a temperature of 10 °C.min<sup>-1</sup> in a range of -80 to 150 °C by DMA. The glass transition temperature was considered based on the  $\tan \delta$  peak.

## 3. Results and discussion

### 3.1. Characterization of particles

The FT-IR spectra of the C/S/S-1 and C/S/S-4 samples are shown in Fig. 2. In this figure, the characteristic

**Fig. 2.** The FT-IR spectra of C/S/S-1 and C/S/S-4 samples.

peaks of poly(methyl methacrylate) and poly(butyl acrylate) can be seen in the C–H covalent bond at 2800–2960  $\text{cm}^{-1}$ , the C–O bond at 1100  $\text{cm}^{-1}$ , and the tensile vibration of the carbonyl group at 1732  $\text{cm}^{-1}$ . The C–C aromatic peak at wavelength 1580  $\text{cm}^{-1}$  corresponds to the benzene ring in polystyrene. The characteristic peak of DVB is in the wave number of 760  $\text{cm}^{-1}$ . These results confirm polymers were formed [22,23].

The DLS curves of C/S/S-1 and C/C/S-4 samples are shown in Fig. 3. As can be seen, the two curves have a narrow distribution indicating that all the latex particles synthesized have narrow distributions. The diameter of the final particle of C/S/S-1 is 80 nm.

TEM images were used to prove the morphology of the C/S/S-1 sample. Fig. 4 shows that the particles have a core/shell structure. The diameters of particles ranged from 80 to 110 nm, with spherical morphology.

### 3.2. The effect of initiator on dynamic-mechanical properties

Although thermal initiators can be applied for

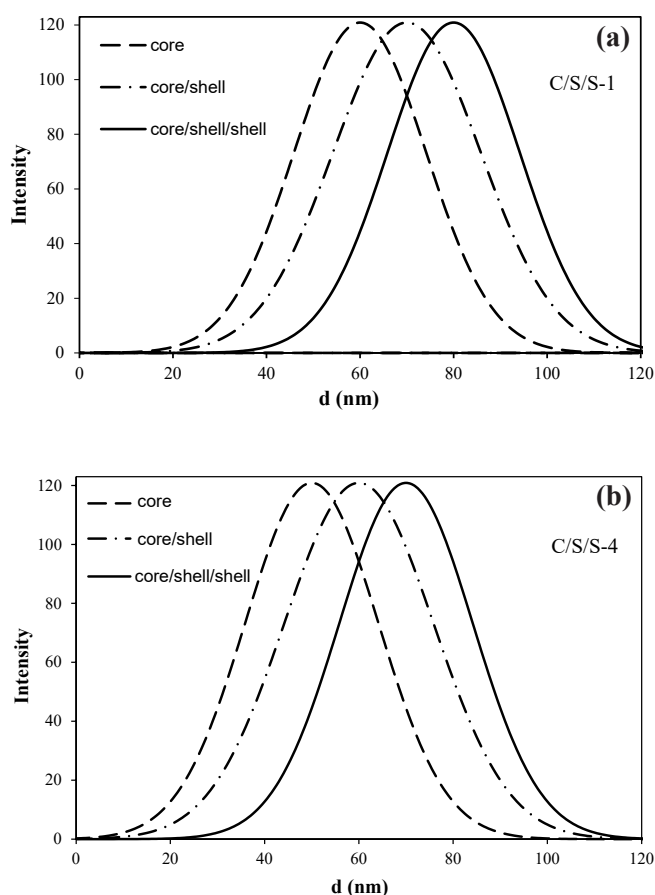


**Fig. 3.** The particle size distributions of multilayer core/shell latex particles of (a) C/C/S-1 and (b) C/C/S-4 samples.

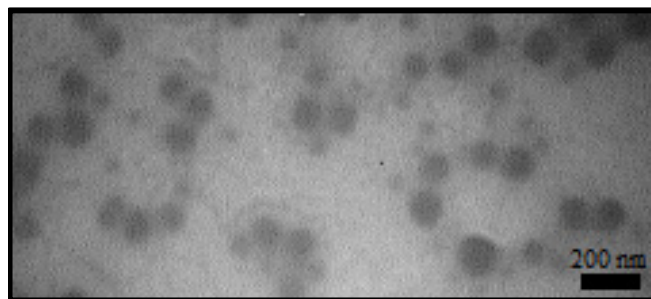


**Fig. 4.** TEM micrograph of C/C/S-1.

polymerization expansion at higher temperatures, their application is limited by the fact that the penetration of rubbery polymer chains into other layers also increased. Therefore, increasing the temperature to lower values is the more practical option to reduce polymer diffusion between layers. Redox initiators should be used at low temperatures because thermal initiators do not produce enough radicals. Polymerization of styrene, methyl methacrylate, and butyl acrylate as the core-shell at ambient temperature with redox initiator is not possible as polymerization is successful at 40°C.

To study the effect of temperature, C/S/S-1 and C/S/S-4 samples were investigated by changing the initiator. According to Table 1 and Fig. 5, the sample with the redox initiator (C/S/S-4) shows a sharp  $\tan\delta$  peak at 67°C, with a height of 0.94, but the sample with the thermal initiator (C/S/S-1) provide a wide effective temperature range for damping. This is because decreasing the polymerization temperature decreases the polymerization rate of butyl acrylate decreases, which enhances the induction period [24]. Also, most of the butyl acrylate is diffused into the core, so the  $\tan\delta$  grows, and its peak is transferred to a higher temperature.

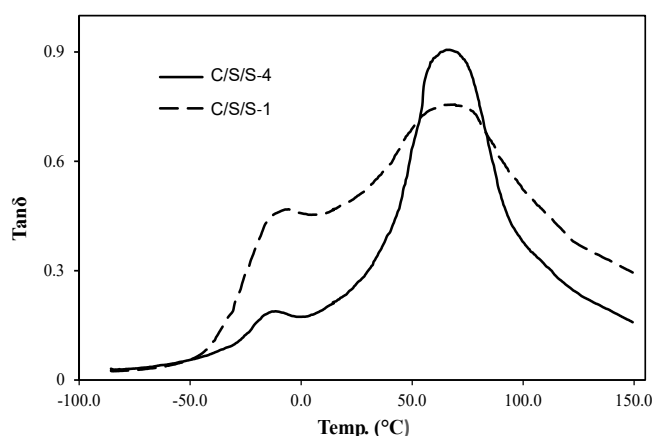


**Fig. 5.** The loss tangent versus temperature curves of C/S/S-1 and C/S/S-4 samples showing the effect of polymerization temperature.

### 3.3. The effect of layer weight ratio on dynamic-mechanical properties

Experimental results show that the weight ratio of the layer of core/shell/shell particles has a profound effect on dynamic-mechanical properties. The  $\tan\delta$ -temperature plots and resulting data for C/S/S-1 (with a layers' weight ratio of 1:2:2), C/S/S-2 (with a layers' weight ratio of 1:2:3), and C/S/S-3 (with a layers' weight ratio of 1:3:3) are illustrated in Fig. 6 and Table 1, respectively. As presented in Table 1, the maximum loss factor and the effective temperature range were significantly enhanced for the C/S/S-2 sample. This may be due to the fact that raising the weight ratio of the outer layer from 1:2:2 to 1:2:3 increased the phase continuity distribution of the core/shell1 region and the peak of core/shell1 considerably. Enhancing the contribution of the outer layer creates bi-continuous morphology and intermediate structures between the layers for numerous reasons, including diffusion of chains together and more swelling. In other words, damping peaks can be transferred to lower temperatures by increasing the shell2 ratio and are improved by using developed intermediate structures. Moreover, the intensity of the graph was probably increased due to more diffusion of soft chains into hard chains, higher friction coefficient, and the mobility of chains.

As the weight ratio of the inner shell (shell 1) (1:3:3) increases, the peaks shift to lower temperatures due to the greater mobility of the soft PBA components and its larger side groups. In addition, soft PBA components easily penetrate PMMA and PS hard components and improve compatibility. Therefore, in general, by

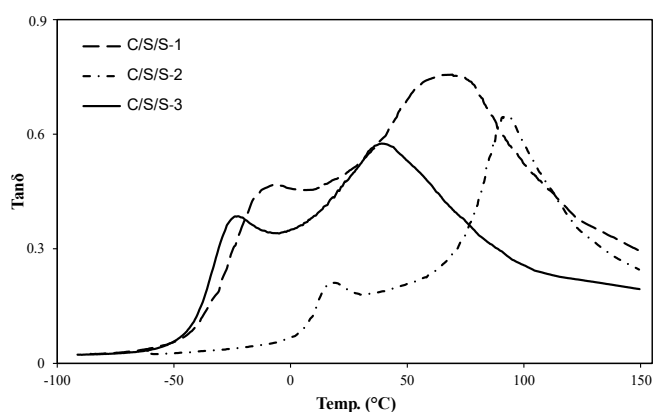


**Fig. 6.** The loss tangent versus temperature curves of C/S/S-1, C/S/S-2, and C/S/S-3 samples showing the effect of weight ratio.

increasing the amount of PBA, the effective damping range increases, and the damping peak shifts to lower temperatures, but its effect is not significant in the middle layers due to the presence of a crosslinking agent and limited movement of the chains.

## 4. Conclusions

In this work, core/shell/shell (C/S/S) particles with PS, P(MMA), and PBA via semi-continuous emulsion polymerization were synthesized. DMA analysis shows that core/shell/shell particles synthesized with a redox initiator have a sharper  $\tan\delta$  peak but a lower effective range of damping than the core/shell/shell synthesized with a thermal initiator.

Two glass transition regions were observed in most of the  $\tan\delta$  diagrams, with a high peak in the core in the first shell region and a small peak in the second shell region. Since the core/shell contains the crosslinking agent, it can be concluded that a complete IPN is formed in core/shell1 and a half IPN in shell1/shell2. It seems that inner layers with DVB form a continuous morphology between layers and only damping the peak, but under different conditions, the outer layer or a part of it shows phase separation.

Changing the weight ratio of the layers and the amount of PBA in the last layer with an increase in the domain phase amount, decrease in domain phase size, and completion of network structures creates bi-continuous morphology, and this core/shell can be easily used for damping at low temperatures.

## References

- [1] M.M. Mazidi, M.K.R. Aghjeh, H.A. Khonakdar, U. Reuter, Structure-property relationships in super-toughened polypropylene-based ternary blends of core-shell morphology, *Rsc. Adv.* 6 (2016) 1508-1526.
- [2] D. Parker, H.J. Sue, J. Huang, A.F. Yee, Toughening mechanisms in core-shell rubber modified polycarbonate, *Polymer*, 31 (1990) 2267-2277.
- [3] J.Y. Qian, R.A. Pearson, V.L. Dimonie, M.S. El-Aasser, Synthesis and application of core-shell particles as toughening agents for epoxies, *J. Appl. Polym. Sci.* 58 (1995) 439-448.
- [4] F. Li, Y. Gao, Y. Zhang, W. Jiang, Design of high impact thermal plastic polymer composites with

- balanced toughness and rigidity: Toughening with core-shell rubber modifier, *Polymer*, 191 (2020) 122237.
- [5] M. Sedki, A. Hefnawy, R.Y.A. Hassan, I.M. El-Sherbiny, Core-shell hyperbranched chitosan nanostructure as a novel electrode modifier, *Int. J. Biol. Macromol.* 93 (2016) 543-546.
- [6] A. Mayer, T. Pith, G. Hu, M. Lambla, Effect of the structure of latex particles on adhesion. Part I: Synthesis and characterization of structured latex particles of acrylic copolymers and their peel adhesion behavior, *J. Polym. Sci. Pol. Phys.* 33 (1995) 1781-1791.
- [7] C. Xu, T. Qiu, J. Deng, Y. Meng, L. He, X. Li, Dynamic mechanical study on multilayer core-shell latex for damping applications, *Prog. Org. Coat.* 74 (2012) 233-239.
- [8] A. Petukhova, A.S. Paton, Z. Wei, I. Gourevich, S. V. Nair, H.E. Ruda, A. Shik, E. Kumacheva, Polymer multilayer microspheres loaded with semiconductor quantum dots, *Adv. Funct. Mater.* 18 (2008) 1961-1968.
- [9] W. Chen, S. Bhaumik, S.A. Veldhuis, G. Xing, Q. Xu, M. Grätzel, S. Mhaisalkar, N. Mathews, T.C. Sum, Giant five-photon absorption from multidimensional core-shell halide perovskite colloidal nanocrystals, *Nat. Commun.* 8 (2017) 15198-15207.
- [10] Y. Su, H. Guo, Z. Wang, Y. Long, W. Li, Y. Tu, Au@Cu<sub>2</sub>O core-shell structure for high sensitive non-enzymatic glucose sensor, *Sensor. Actuat. B-Chem.* 255 (2018) 2510-2519.
- [11] D. Klemperner, *Advances in interpenetrating polymer networks*, CRC Press, 1994.
- [12] D. Klemperner, L.H. Sperling, L.A. Utracki, *Interpenetrating polymer networks*, American Chemical Society, Washington, DC (United States), 1994.
- [13] L.A. Utracki, B.D. Favis, *Polymer alloys and blends*, *Handbook of Polymer Science and Technology*, vol. 4, 1989, pp. 121-185.
- [14] L.H. Sperling, T. Chiu, D.A. Thomas, Glass transition behavior of latex interpenetrating polymer networks based on methacrylic/acrylic pairs, *J. Appl. Polym. Sci.* 17 (1973) 2443-2455.
- [15] J. D. Zhang, M. J. Yang, Y. R. Zhu, H. Yang, Synthesis and characterization of crosslinkable latex with interpenetrating network structure based on polystyrene and polyacrylate, *Polym. Int.* 55 (2006) 951-960.
- [16] L.H. Sperling, J.J. Fay, Factors which affect the glass transition and damping capability of polymers, *Polym. Advan. Technol.* 2 (1991) 49-56.
- [17] J.A. Grates, D.A. Thomas, E.C. Hickey, L.H. Sperling, Noise and vibration damping with latex interpenetrating polymer networks, *J. Appl. Polym. Sci.* 19 (1975) 1731-1743.
- [18] L.H. Sperling, *Synthesis of IPNs and Related Materials*, in: *Interpenetrating Polymer Networks and Related Materials*, Springer, Boston, MA (United States), 1981, pp. 65-103.
- [19] F. Zahedi, I.A. Amraei, M.A. Fathizade, Investigation of dynamic-mechanical properties of multilayer latex IPNs (MLIPNs) with core/shell morphology: Synthesis and characterization, *Polymer*, 83 (2016) 162-171.
- [20] M.S. Silverstein, Interpenetrating polymer networks: So happy together?, *Polymer* 207 (2020) 122929.
- [21] P.C. Hiemenz, T.P. Lodge, *Polymer chemistry*, 2<sup>nd</sup> ed., CRC press, 2007.
- [22] L.Y. Wan, L.P. Chen, X.L. Xie, Z.P. Li, H.Q. Fan, Damping properties of a novel soft core and hard shell PBA/PMMA composite hydrosol based on interpenetrating polymer networks, *Iran. Polym. J.* 20 (2011) 659-669.
- [23] E. Tang, M. Yao, P. Du, M. Yuan, S. Liu, Synthesis and dynamic mechanical study of core-shell structure epoxy/polyacrylate composite particle, *J. Polym. Res.* 23 (2016) 204.
- [24] G. Wu, C. Wang, Z. Tan, H. Zhang, Effect of temperature on emulsion polymerization of n-butyl acrylate, *Procedia Engineer.* 18 (2011) 353-357.